*Coastal Dynamics 2017*
*Paper No. 176*

# MONITORING NEARSHORE PROCESSES AND UNDERSTANDING SIGNIFICANT COASTAL CHANGE USING X-BAND RADAR

John Atkinson[1], L.S. Esteves[1], J.J. Williams[2], P.S. Bell[3], D. McCann[3]

## Abstract

Remote sensing through X-band radar can provide wave and current parameters and bathymetric maps in a 4-km radius from a land-based deployment. This paper explores the use of radar to monitor changes in nearshore bathymetry at Thorpeness, Suffolk, UK. The method presented enables significant nearshore changes to be identified based on the analysis of standard deviation of sediment volume. Seasonal changes in bathymetry can reach 4 m but depths tend to be consistent in each season. A storm power index was calculated for periods of time preceding the significant changes in bathymetry. Results indicate that impact on the nearshore is not directly linked to storm power. Storm clusters and antecedent nearshore conditions seem to be important factors, as larger volume changes were measured as a result of the first and smallest storm of a cluster.
**Key words:** sediment transport, storm impact, nearshore, bathymetry, remote sensing.

## 1. Introduction

Understanding interactions between the nearshore and shoreline are integral to gaining a more complete understanding of the physical dynamics of a coastal system and how significant change is caused. Significant erosion events are often identified based on a storm threshold defined per metocean conditions (e.g. exceedance of certain significant wave height and duration). Although the storm threshold method may capture events with the highest energy and, therefore, the most probable significant impact at the coast; it can miss the effect of persistent, moderate conditions or clustered lower energy events (Dissanayake *et al*., 2015).

Preferably, studies aiming to assess storm impact at the coast should be based on quantifications of change, such as in beach volume, cliff retreat or nearshore bathymetric changes. Traditional methods used for the collection of bathymetric data in the nearshore are expensive and time consuming, making them unsuitable for regular monitoring. Due to these difficulties, there is a scarcity of data at spatial and temporal resolutions (Coco *et al.,* 2014) that would allow quantification of impact from both high energy events and lower energy clusters.

Remote sensing technologies offer a viable alternative for longer-term high frequency coastal monitoring of large areas. X-band radar systems can be employed to derive wave parameters, nearsurface currents (Reichert *et al*., 1999), bathymetry (Bell, 1999) and intertidal topography (Bell *et al*., 2016) during day and night within a 4-km radius of the system. This paper presents preliminary results from research aiming to test whether X-band radar technology can be used as a coastal monitoring tool to support evidence-based coastal management decisions. An X-band radar was installed in Thorpeness (Eastern England) in the period August 2016 to April 2017. The research uses a combination of X-band radar and fieldwork data to quantify nearshore and beach changes in a mixed sand and gravel system, and understand their temporal and spatial variability and the associated driving conditions. The objective here is to demonstrate how X-band radar data can be used to quantify seasonal and storm-driven changes in nearshore bathymetry.

### *1.1 Study Area*

Thorpeness beach (Figure 1, 52.1823°N, 1.6130° E) is an eastward facing, mixed sand and gravel beach (MSGB) in Suffolk, UK. The study area extends between the ness (a cuspate shingle foreland) in the north

[1] Life and Environmental Sciences, Bournemouth University, Bournemouth, UK. atkinsonj@bournemouth.ac.uk
[2] Mott MacDonald, 8-10 Sydenham Road, Croydon, UK
[3] National Oceanography Centre, Liverpool, UK

to the south end of the Thorpeness village. Southwards from the Ness the MSGB is backed by Pleistocene soft cliffs of weakly cemented poorly sorted coarse sands.


Figure 1. Location of Thorpeness in East England (right panel, Digimap, 2017) and photos of the beach, facing south from the north of the radar position (top left panel), and facing north from the center of the village seafront (bottom left)

The underlying bathymetry and resulting physical dynamics are complex. To the north of the Ness the Sizewell bank acts as a sink for fine and medium sand from the north and south (Carr, 1979). This in turn is influenced by the underlining Pliocene geology of the Coralline Crag formation (cemented fine sands and silts rich in bryozoan and bivalve shells formed in a shallow shelf environment). The Crag forms an underwater ridge of around 12 km long and 2 km wide which outcrops in the Aldeburgh area (Long and Zalasiewicz, 2011) extending SW-NE offshore from Thorpeness (Pye and Blott 2006).

The wave climate is dominated by NE or SE wave direction varying year to year. The tidal regime is semi-diurnal mesotidal (peak astronomical range ~2.5 m). Historical erosion and flooding events are often associated with the large winter storm surges, reaching 3.78 m in Aldeburgh (Lamb *et al*., 2005). Two recent erosion events (2010 and 2013) caused threats to beach front properties and instigated private and public funded coastal protection. The radar data used in this research were obtained as part of the X-Com project (funded by the Natural Environment Research Council/UK), which is supported by the local authority (Suffolk Coastal District Council), Mott MacDonald and local residents. The local authority wants to better understand the complex interactions between sediment movement and shoreline change to inform coastal management decisions.

## 2. Methods

### *2.1 Radar Overview*

X-band radar is defined by IEEE (Institute of Electrical and Electronics Engineers) as microwave energy within the frequency of 8 and 12 GHz and wavelength of 2.50 to 3.75 cm. It has been traditionally used for nautical navigation and collision avoidance. In the late 20th century Young *et al*. (1985) derived a method for extracting sea state parameters, surface currents and water depth from X-band radar data.

The wavelength allows resolving relatively small surface ripples (caused by wind speeds >3 m $s^{-1}$) on the water surface through an understanding of Bragg scattering (Bragg, 1913). The reflection of these radar

pulses causes constructive interference which is received by the radar and the signal strength can be used to understand the size and shape of the ocean surface. The radar system deployed at Thorpeness consisted of a Kelvin Hughes 10kW, 9.8 GHz which was digitized through a OceanWaves WaMoS II analogue to digital converter providing ~0.8-degree horizontal resolution.

Wave parameters from the radar were derived through the WaMoS II radar system; this calculates a range of wave period, direction, spreading and height values based on Bragg scattering of the transmitted radar pulses. To accomplish this for each record, an image sequence of radar return intensity values is taken from the central area of the radar view (200 x 200 m). The processing procedure within WaMoS II to derive these parameters is well documented within literature (Reichert *et al*., 1999; Hessner *et al*., 2014).

A bathymetric inversion was used to calculate water depth at 60 $m^2$ cells within the radar view utilizing the digitized images from the WaMoS system. The bathymetric inversion is dependent upon wave conditions, specifically the wave length and period of the waves at site being influenced by the sea bed (Bell and Osler, 2011). It applies the dispersion relation between wave frequency (σ), wave number (*k*) and mean water depth (h). Within a region defined by σ, the mean water depth directly affects k. To calculate these wave parameters analysis of a finite area of water surface (large enough to cover at least one wavelength in all directions) is undertaken with the assumption that the area is homogenous for both *k* and frequency spectra. This technique is further explained in Bell (2009a; 2009b). To reduce computing time, data processing focused on a selected area of 3.3 $km^2$ (1500 m by 2200 m) shown in Figure 2.

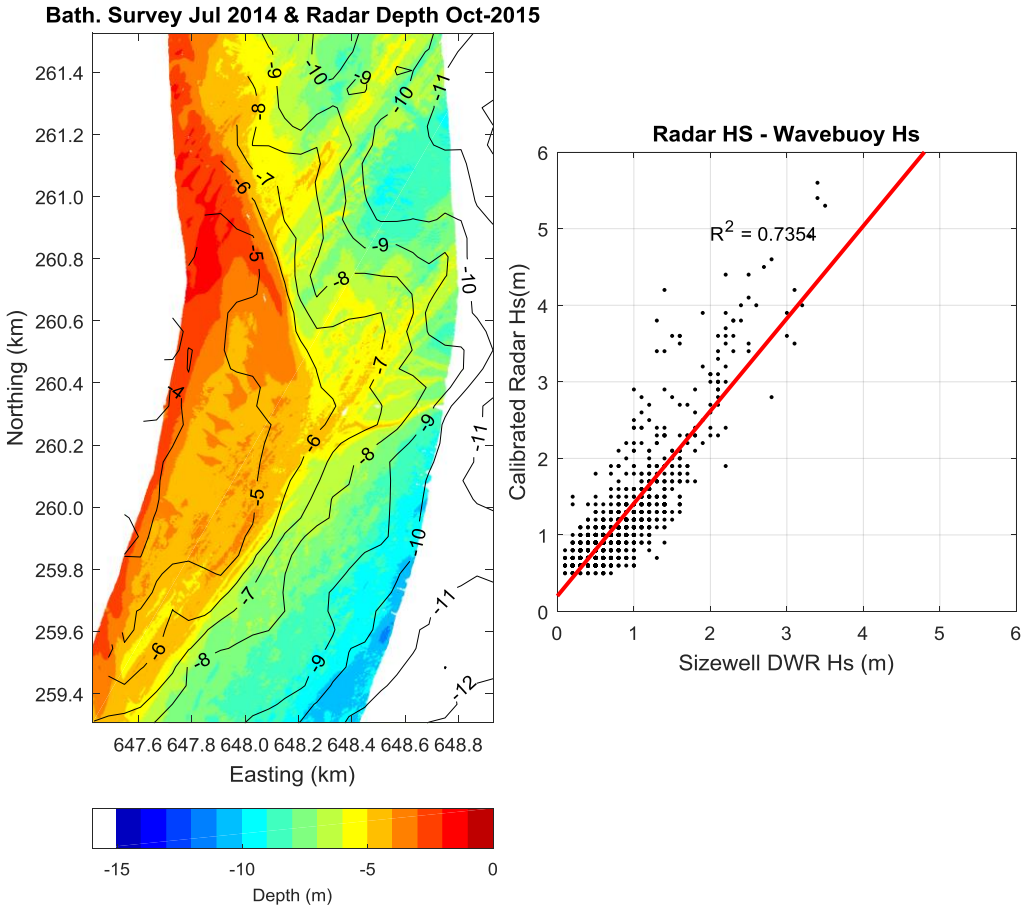


Figure 2. Multibeam bathymetry survey with overlaid radar derived bathymetric map (left panel), radar derived wave height (calibrated) against wave buoy data (right panel)

### *2.2 Calibration and Validation*

Due to non-linearity of the radar imaging mechanism, wave height cannot be directly inferred from raw data (Borge et al. 1999). However a calibration can be applied through coincident wave measurements

from another instrument based on the method outlined in Alpers and Hasselmann (1982, equation 1). In this case a wave buoy located ~1900 m North and ~3500 m East (Cefas Sizewell Datawell Waverider) of the radar position provided a significant wave height (Hs) time series from which to calculate the calibration coefficients in equation 1 (Figure 2, right panel).

$$H_s = A + B\sqrt{SNR} \tag{1}$$

Where A is the intercept and B the slope of the fit between SNR and calibrated Hs.

Validation of the depth data during the radar deployment will be based upon a multibeam bathymetric survey performed in late January 2017. Initial checks were made through comparison of a multibeam survey from July 2014 (Figure 2, left panel) which shows strong correlation of the major features observed; the concurrent data however can be used to more accurately define error and uncertainty from the radar derived depths.

### 2.3.1 *Longer-term Change in bathymetry and sediment volume*

To understand the variability in nearshore bathymetry at a seasonal scale, data analysis focused on identifying the maximum and minimum nearshore depths measured between September 2015 and November 2016. The baseline used to estimate sediment volume changes was defined as the deepest mean depth within the radar view area observed in the period. It is assumed that at its deepest state the area would have the least amount of sediment. The deepest mean depth was observed in November 2016 and this was considered the baseline condition (0 $m^3$) from which to calculate minimum, mean and maximum sediment volume changes. Table 1 shows the estimated sediment volume gain in each given period in relation to the baseline. To illustrate the variance in depth within the radar view, two profiles were taken as an offshore extension of UK Environment Agency (EA) beach profiles, which coincide with some of the most dynamic areas in the radar view (Figure 3).

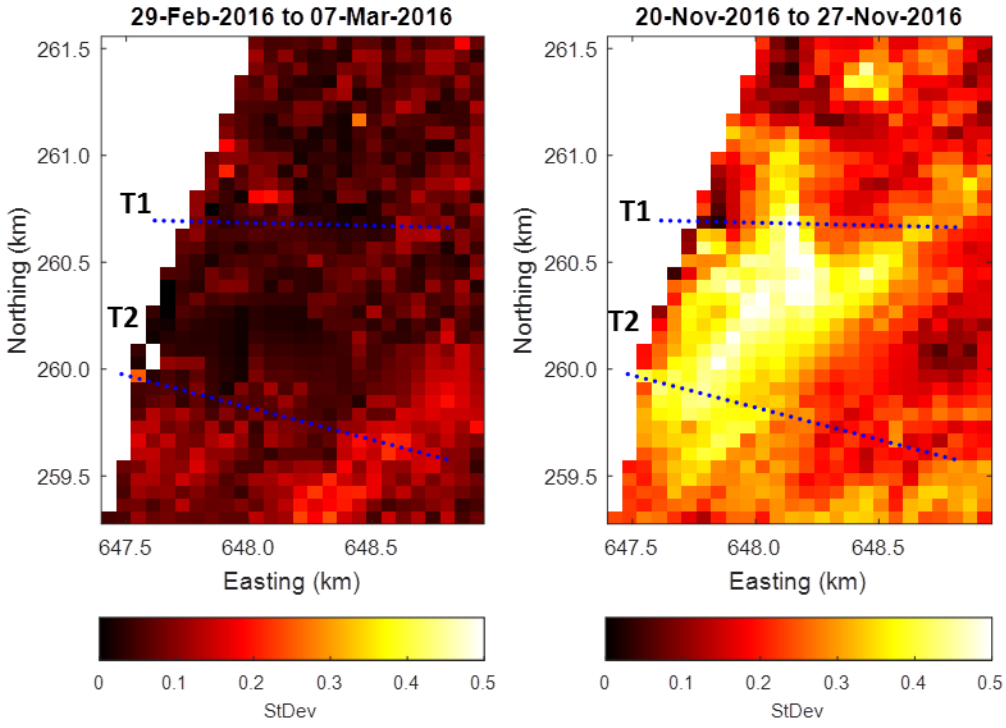


Figure 3. Seven-day standard deviation of each pixel during low variance (left panel) and high variance (right panel) showing EA profile positions (dotted blue lines)

2.3.2 *Shorter Term Change in bathymetry*
Periods of rapid change were identified through evaluation of the highest standard deviation in the depth at each pixel within an arbitrary period of time (7 days in this case). Figure 3 shows examples of periods of high and low variation. To identify periods of change a peak finding algorithm was implemented based upon an exceedance of 0.2 m standard deviation in 7 days of consecutive records. If the data reflecting high standard deviation passed quality checks, volume changes were calculated for each pixel and the metocean conditions preceding the period of significant change were characterized to identify whether the changes resulted from: (a) single high energy significant event; (b) clustered events; or (c) persistent conditions. Storm events here were identified using the thresholds of Hs ≥1.5 m and duration >6 hours. To quantify the relative energy of these storm events the 'storm power index' ($S_{pi}$) was calculated using equation 1 (Dissanayake et al., 2015), where $D$ = Duration threshold, $H$ = Significant wave height threshold :

$$S_{pi} = \sum_{i=1}^{n} (\Delta D \times \Delta H_i^2) \quad (2)$$

## 3. Results

### 3.1. *Longer-term Changes*

Table 1 presents the minimum, maximum and mean sediment volume gain in relation to the baseline (Nov 2016) within the 3.3 km$^2$ study area by month and season and respective data return in percentage of time. Low data return in the periods March-May 2016 and October 2016 was due to radar technical problems.

Table 1. Maximum, mean and minimum volume monthly and seasonally from September 2015 to November 2016 extracted from X-band radar data with corresponding data return

| **Time period** | **Volume (m$^3$)** | | | **Valid Data Return (%)** |
|---|---|---|---|---|
| | **Max volume** | **Mean volume** | **Min volume** | |
| Sep 15 | 112562 | 85805 | 76262 | 97 |
| Oct 15 | 101364 | 65221 | 44717 | 99 |
| Nov 15 | 88712 | 54181 | 41918 | 9 |
| Dec 15 | 48737 | 31424 | 15840 | 21 |
| Jan 16 | 24178 | 20039 | 16322 | 7 |
| Feb 16 | 44614 | 24747 | 7526 | 65 |
| Mar 16 | 36686 | 32968 | 30545 | 18 |
| Apr 16 | - | - | - | 0 |
| May 16 | 46248 | 39152 | 33932 | 24 |
| Jun 16 | 88642 | 62292 | 35831 | 99 |
| Jul 16 | 85394 | 49309 | 31869 | 59 |
| Aug 16 | 103706 | 61455 | 47431 | 94 |
| Sep 16 | 66797 | 56052 | 34863 | 93 |
| Oct 16 | - | - | - | 0 |
| Nov 16 | 58675 | 35247 | 0 | 94 |
| Sep-Nov 15 (Autumn) | 112562 | 68757 | 41918 | 60 |
| Dec 15-Feb 16 (Winter) | 48737 | 25923 | 7526 | 30 |
| Mar-May 16 (Spring) | 46248 | 36457 | 30545 | 14 |
| Jun-Aug 16 (Summer) | 103706 | 58881 | 31869 | 84 |
| Sep-Nov 16 (Autumn) | 66797 | 47513 | 0 | 62 |

Data shown in Table 1 and Figure 4 suggest that sediment volumes are largest in the summer and decrease throughout the autumn to reach minimum values in the winter. Interestingly, it seems that sediment mobility (indicated by the difference between maximum and minimum volumes observed in each period) is also highest in the summer and autumn months and changes are less pronounced over the winter and spring (Figure 4). This observation needs to be considered carefully as during the winter months in 2015 data

return was low. The volume changes are indicated here to enable relative comparison of sediment mobility across the study area in each month and season and do not refer to the direction of change (erosion or deposition) in each period. Erosion and deposition trends vary spatially and this analysis is ongoing.

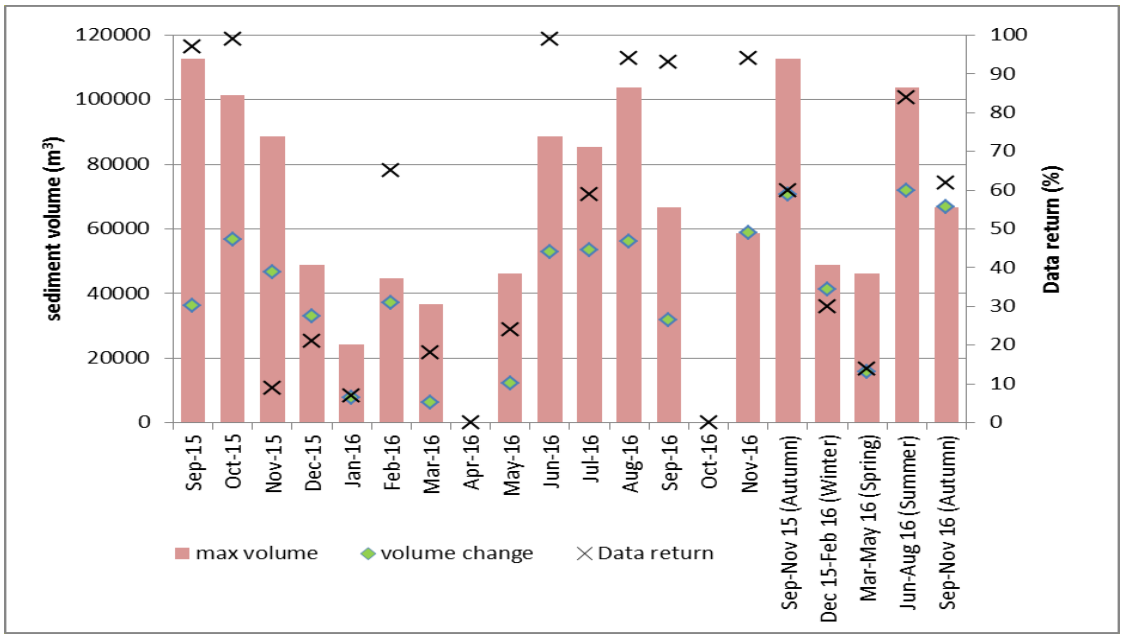


Figure 4. Maximum volume of sediment gained in relation to the baseline (November 2016), maximum volume change in each month and season and respective data return

Figure 5 shows bathymetric contours derived from radar data obtained in 30th September 2015, 9th February, 19th August, 26th November 2016 used here to illustrate seasonal variations. This figure shows a large shallower area (depth<5 m) extending from the SW in September 2015 and August 2016, which is not evident in February and November 2016. The changes in bathymetry between the dates shown in Figure 5 are displayed in Figure 6. The radar data suggests considerable bathymetry changes reaching 3-4 m within the nearshore (Figure 6). These changes seem to indicate the development of an oblique bar in the spring and summer (accretion from February 2016 to August 2016) and its erosion in the autumn and winter (erosion from September 2015 to February 2016 and from August 2016 to November 2016). Magnitudes of change are reduced away from this area and can be minimal at the north and south of the study site. The orientation and position of the 'bar' and the areas of largest changes seem to follow the Coralline Crag ridge present in the study area. It is possible to infer that the underlying geology has an important effect on the morphology and evolution of nearshore sedimentary features.

To further understand the seasonal changes, depth was extracted along two transects (T1 and T2), which are extensions of EA beach profiles. Figure 7 shows the bathymetric profiles extracted from the data collected at the four dates shown in Figure 5 and the standard deviation at each pixel calculated based on all data (from September 2015 to November 2016). The standard deviation plot indicates that T2 crosses an area of largest depth variability than T1, which is also evident when comparing the respective profiles. The depth profiles shown along transects T1 and T2 indicate clear variations between seasons, with accreted (shallower) profiles in September 2015 and August 2016 and eroded (deeper) profiles in February and November 2016. In T2 summer accretion of up to 4 m is pronounced in the nearshore (up to 500 m offshore), while in T1 accretion (~3 m) is more pronounced further offshore (700-1100 m). This difference reflects the SW-NE orientation of the oblique bar, which seems to reduce in size northwards. Particularly along T2, the seasonal signal is striking, with 'summer' and 'winter' profiles showing very similar shape and depths. Along both transects, the evident increase in slope at 500-600 m distance offshore may be an effect of the underlying geology, which is likely to control the position of the oblique bar.

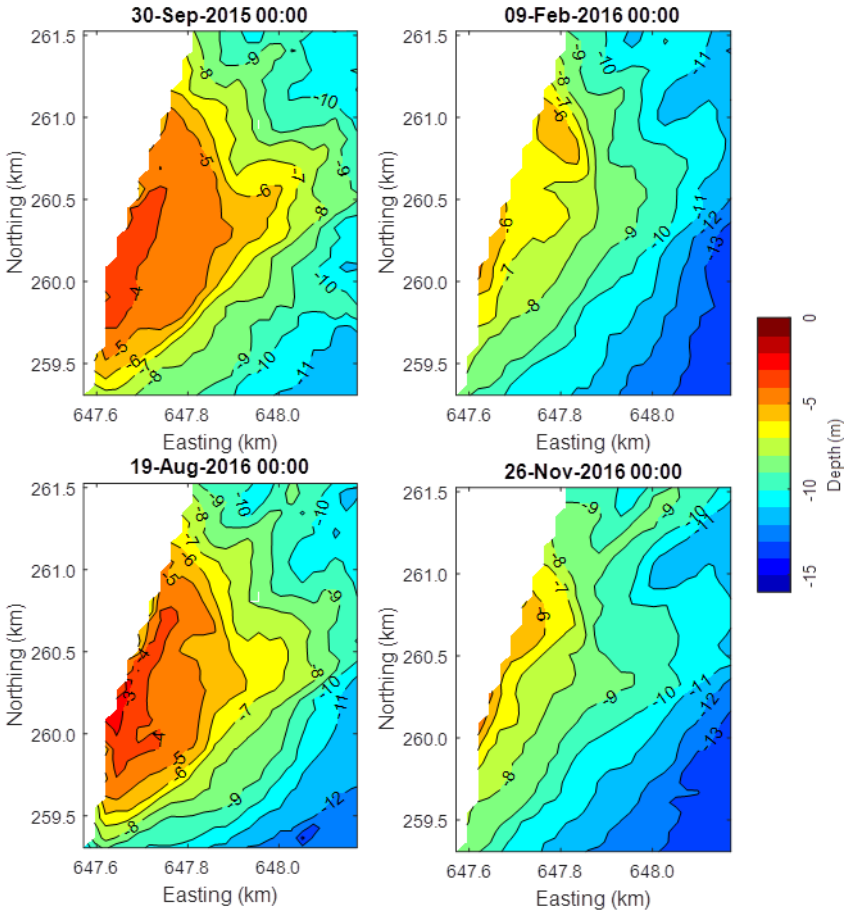


Figure 5. Radar derived bathymetric contours observed during deployment.

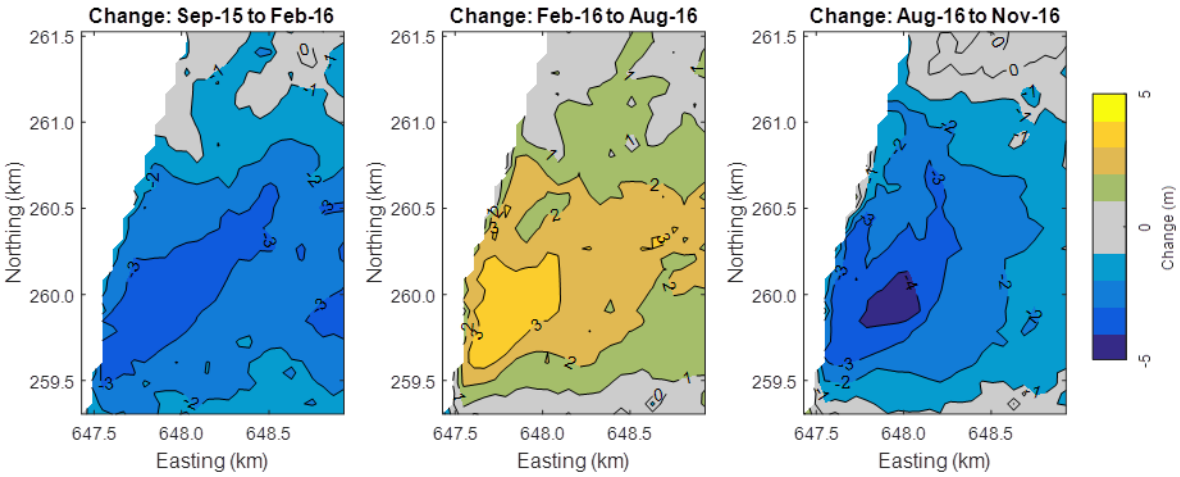


Figure 6. Observed change between the seasonal maxima and minima.

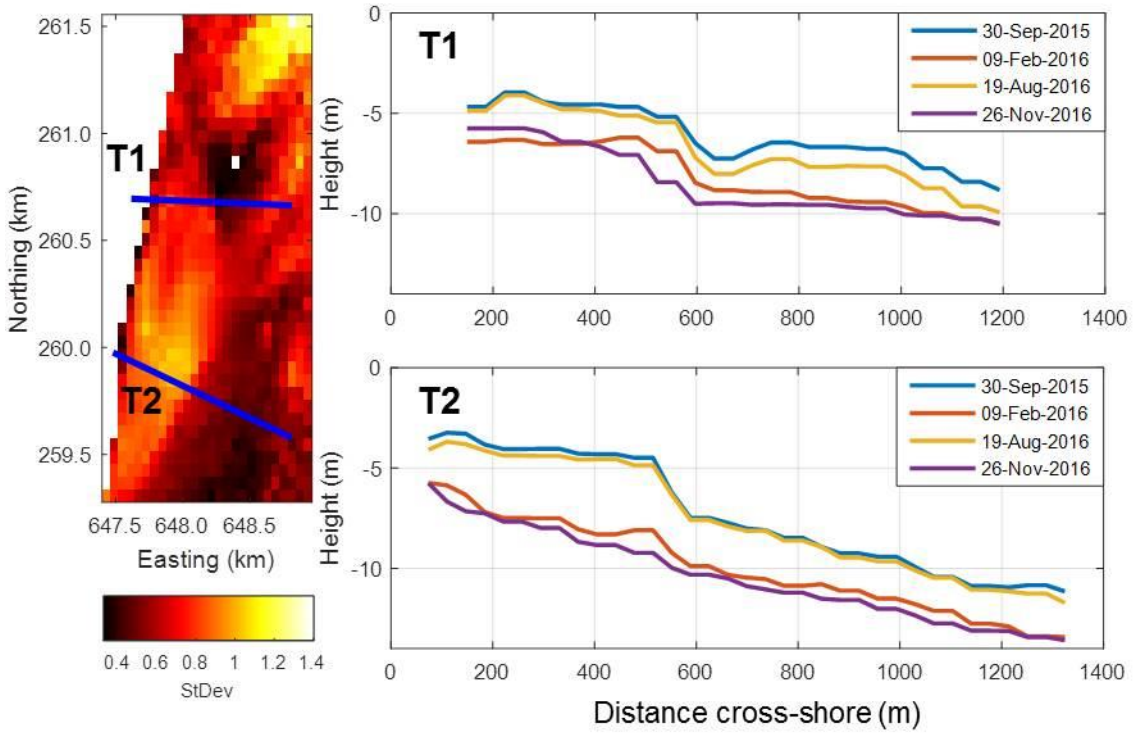


Figure 7. Standard deviation of each pixel between 30th September 2015 and 26th November 2016 (left panel) and the radar derived depth along the transects T1 and T2 (right panels)

### *3.2 Short-term changes*

The analysis of short-term changes (arbitrarily identified as the highest standard deviation of depths in a seven-day time span) indicated that the largest recorded changes were observed in the period 20th to 27th November 2016. During this period, a cluster of three individual storms was observed as indicated by the wave parameters shown in Figure 8. The first two storms approached from the SE with peak Hs of 3.1 m and 3.3 m, respectively. The third storm, approached from the NE with peak Hs = 3.1 m. Table 2 presents the times, $S_{pi}$ and resulting change in the radar view due to the three identified, clustered storms. These data indicate that the first storm had the lowest $S_{pi}$ but resulted in both the largest sediment volume change per hour and total change over the storm duration, Storm 2 and 3 although longer in duration resulted in less volume change per hour and in total.

Figure 9 shows the standard deviation over the period and the depth profiles along transects T1 and T2 at four selected dates during the period of the clustered storms of 20th – 27th Nov 2016. The first storm (20th-21st November) approached from the SE and have resulted in the largest changes in sediment volume across the study area (Table 1), which along T1 the most pronounced erosion (>1 m) was observed in the most offshore part of the profile (800-1200 m offshore) and along T2 erosion was observed more evenly along the profile from the nearshore up to 800 m offshore.. The second southerly storm (22nd-23rd November) caused relatively little impact on T1 whereas erosion was observed along T2 between 100 m and 600 m offshore (although of lower magnitude than in the previous storm). Storm 3 (24th-26th November) approached from the NE and have caused the largest impact (erosion exceeding 1 m) in the nearshore of T1 (between 300 and 600 m) and little change elsewhere. .

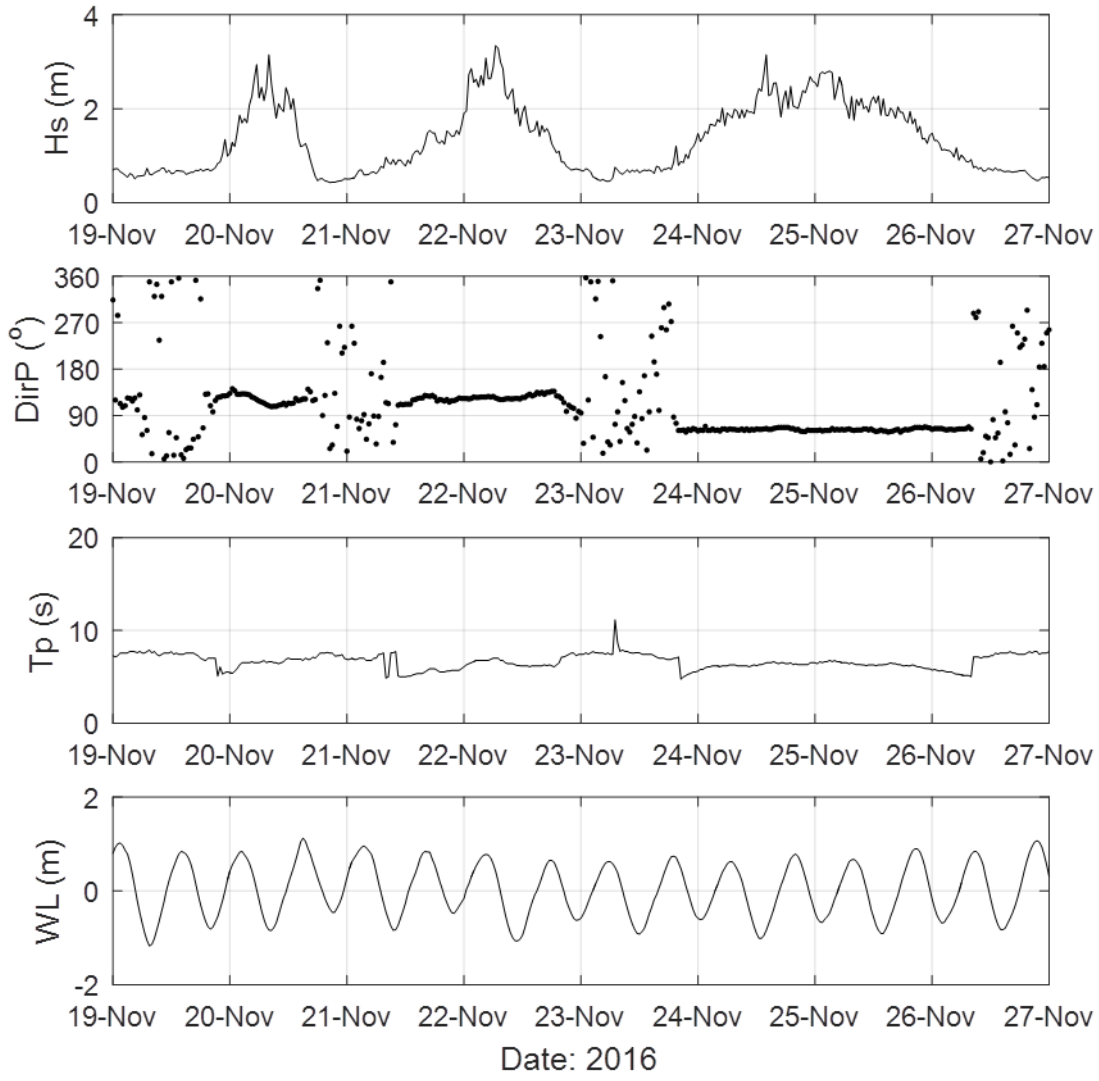


Figure 8. From top to bottom the panels show radar-derived significant wave height (Hs), peak period direction (DirP), peak period (Tp) and water level (WL) for the period 19th to 27th November 2016.

Table 2. Storm timings, storm power index ($S_{pi}$) and associated sediment volume changes in the nearshore of the study area for three clustered storms in November 2016

| **Storm** | **Storm Time Start** | **Storm Time end** | **$S_{pi}$** | **Volume Change Radar View ($m^3$)** | **Volume changes ($m^3$/h)** |
|---|---|---|---|---|---|
| 1 | 20-Nov-2016 02:00 | 20-Nov-2016 13:30 | 59.39 | -20536 | 1785.74 |
| 2 | 21-Nov-2016 23:30 | 22-Nov-2016 13:00 | 86.13 | -9737 | 721.26 |
| 3 | 24-Nov-2016 02:30 | 25-Nov-2016 20:30 | 200.57 | -10823 | 257.69 |

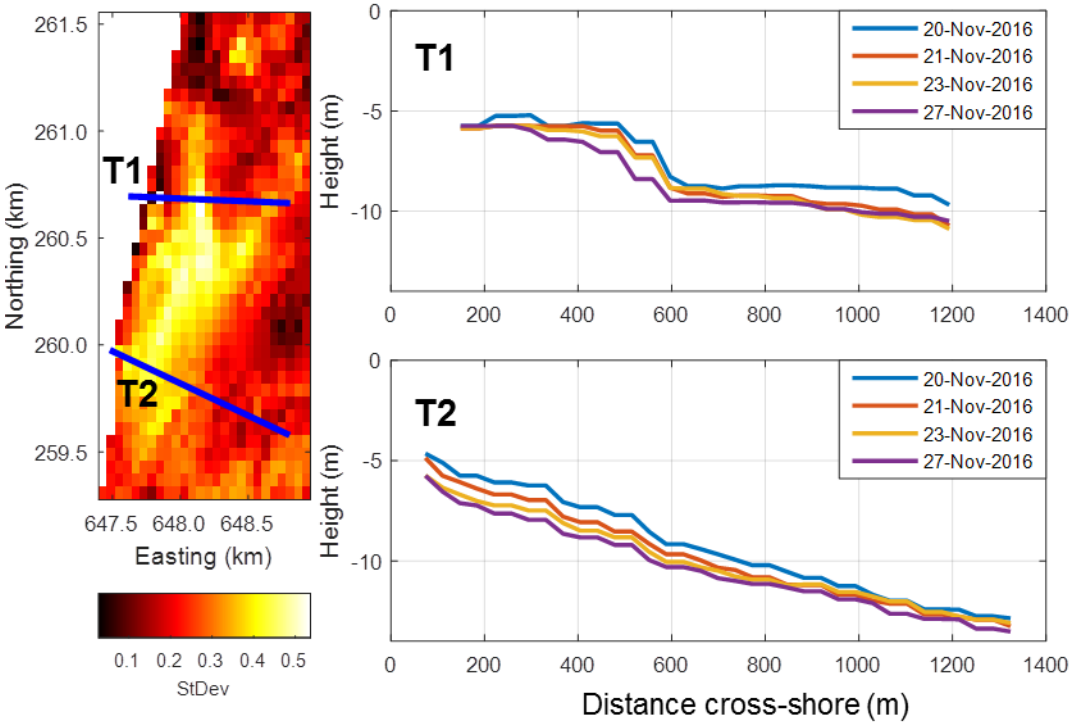


Figure 9. Standard deviation of radar pixels between 19th and 27th November, with location of nearshore transects (left panel) along which depths were extracted for the selected dates (top and bottom right panels)

**Discussion**

Feedback between hydrodynamics and bathymetry is a key element to the nearshore system dynamics and variability (Holman and Stanley, 2007) and radar goes someway to characterize all the essential parameters. It is however limited by resolution and uncertainty within the system which need to be understood before making assumptions on the behaviour observed. The wave parameters are shown to have strong agreement with wave buoy measurements ($R^2$ = 0.74), although radar derived wave height has been found to have an overestimation of young wind seas and underestimation of long swells (Carrasco *et al.*, 2016) with a general accuracy given as Hs±10% (Reichert *et al.*, 1999). When employing methodology based upon observed change during events with Hs exceeding 3 m this precision is adequate for an understanding of the driving forces.

For some practical and research applications, the resolution of the grid and the accuracy in which bathymetry is resolved cannot compete with traditional *in situ* methods. For applications requiring an understanding of variability in large areas and over a range of time scales, the radar offers unmatched cost-benefit, especially in locations where wave conditions are at least moderate and bathymetric changes are considerable. Traditional survey techniques (single or multibeam echo-sound) are limited by survey regularity and conditions preventing data collection. Argus video monitoring systems have shown accuracy of ~10% of the local depth to a range of ~1000 m (Bergsma *et al*. 2016). However, video systems are limited by daylight hours, visibility due to weather conditions and require geometry corrections if wind or other factors result in movement of the cameras. The use of radar allows the long-term monitoring of the nearshore which results in a continuous (24 hours a day) record of bathymetric change and therefore the opportunity to capture significant change over smaller time scales. The impact of an event on the nearshore can be captured without the need for planned or quick response surveying. The seasonal and short term analyses have demonstrated the potential of X-band radar to characterize behaviour at a range of temporal scales in the nearshore.

At Thorpeness, the radar captured seasonal bathymetric changes of 3-4 m and helped understand the variability of sediment volume changes in space and across a range of time scales. Seasonal changes are large, but seem to fully recover, resulting in well-defined seasonal conditions (e.g. the presence of an

oblique bar in late summer/early autumn, which is absent in late autumn/winter). The spatial variations are likely to result from a combination of control exerted by the underlying geology and prevailing wave direction, although this needs to be explored further.

In the short term the most prominent observation presented is that a high storm index ($S_{pi}$) does not necessarily result in a large sediment volume change in the nearshore. Other factors, such as the direction of waves, the effect of storm clusters and the condition of the area (eroded or accreted) at the time of the storm, are likely to play a role on nearshore changes. The effect of storm clustering on beach profiles has been documented. Karunarathna *et al.* (2014) concluded that storm clustering on a sandy beach was seen to increase erosion when compared to a single event of similar $S_{pi}$. Dissanayake *et al*. (2015) found that the foreshore was affected greatest by the initial storms, which then allowed greater energy of the latter storms to increase erosion in the upper part of the beach. This may be a plausible explanation for the results reported here. However, further investigation, including comparison of other storm events (single and clusters), is required.

Wave direction has been observed to have varying impacts on the north and south transects in the short period presented. This variance needs to be investigated further to understand the effects of a bimodal wave climate at site, particularly the effect of persistent events from the north or south and how this persistence may change the nearshore and shoreline year to year.

## 5. Conclusions

This paper focuses on the use of bathymetric maps derived from wave inversions and proposes a relatively simple method to identify period of significant change. The data and methods presented in the paper have shown the utility of radar as a monitoring system of nearshore processes. The radar data obtained at Thorpeness (Suffolk, East England) captured seasonal changes in nearshore bathymetry of up to 4 m of accretion in the late summer/early autumn in relation to the winter). Conditions seem to fully recover resulting in a well-defined seasonal signal. The method was also applied for shorter-term monitoring (e.g. the effects of storms). Preliminary results suggest that high energy storms do not necessarily result in the largest nearshore changes; these may be influenced by the direction of the waves and antecedent conditions (i.e. how eroded or accreted the area is at the time the storm strikes). Spatial variation is likely to be influenced by underlying geology and wave direction. This paper has gone some way in characterising the complexity of the site and as more data becomes available (after processing of radar data and assimilation of surveyed beach topography) further conclusions can be drawn.

## Acknowledgements

X-band radar and evidence-based coastal management decisions (X-Com) was funded by the Natural Environment Research Council (NERC, reference NE/M021564/1). John Atkinson would like to thank Bournemouth University, Suffolk Coastal District Council and Mott MacDonald for funding his PhD studentship.

## References

Alpers, W. & Hassellmann, K., 1982, Spectral signal to clutter and thermal noise properties of ocean wave imaging synthetic aperture radars. *International Journal of Remote Sensing*, (3), 423–446

Balson, P.S., Mathers, S.J., Zalasiewicz, J.A., 1993. The lithostratigraphy of the Coralline Crag (Pliocene) of Suffolk. *Proceedings of the Geologists' Association* 104, 59–70

Bell, P. S., 1999. Shallow water bathymetry derived from an analysis of X-band marine radar images of waves. *Coastal Engineering*, 37 (3–4), 513–527.

Bell, P. (2009a) Coastal mapping around shore parallel breakwaters. *Hydro International*, 13 (1), 18- 21.

Bell, P. (2009b) Remote bathymetry and current mapping around shore-parallel breakwaters. *In: 33rd IAHR Congress - Water Engineering for a Sustainable Environment*, Vancouver, August 9-14

Bell, P. & Osler, J., 2011, Mapping bathymetry using X-band marine radar data recorded from a moving vessel. *Ocean Dynamics*, 61 (12). 2141-2156.

Bell, P. S., Bird, C. O. and Plater, A. J., 2016. A temporal waterline approach to mapping intertidal areas using X-band marine radar. *Coastal Engineering*, 107 , 84–101.

Bergsma, E. W. J., Conley, D. C., Davidson, M. A. and O'Hare, T. J., 2016. Video-based nearshore bathymetry estimation in macro-tidal environments. *Marine Geology*, 374 , 31–41.

Bragg, W. H. and Bragg, W. L., 1913. The Reflection of X-rays by Crystals. *Proceedings of the Royal Society of*

*London. Series A* [online], 88 (605), 428 LP-438.

Carr, A. P., 1979. Sizewell-Dunwich Banks field Study, Long-term changes in the coastline and offshore banks, *Institute of Oceanographic Science Report*, (89), 1-24.

Carrasco, R., Streßer, M., and Horstmann, J., 2016. A Simple Method for Retrieving Significant Wave Height from Dopplerized X-Band Radar. *Ocean Science Discussions* [online], (May), 1–14. Available from: http://www.ocean-sci-discuss.net/os-2016-29/.

Coco, G., Senechal, N., Rejas, A., Bryan, K. R., Capo, S., Parisot, J. P., Brown, J. A., and MacMahan, J. H. M., 2014. Beach response to a sequence of extreme storms. *Geomorphology* [online], 204, 493–501.

Davidson, M., Van Koningsveld, M., de Kruif, A., Rawson, J., Holman, R., Lamberti, A., Medina, R., Kroon, A. and Aarninkhof, S., 2007. The CoastView project: Developing video-derived Coastal State Indicators in support of coastal zone management. *Coastal Engineering*, 54 (6-7), 463–475.

Digimap, 2017, GB Overview, Scale 1:8,000,000, Using: EDINA *Digimap Ordnance Survey Service*, Created*:* March 2017.

Dissanayake, P., Brown, J., Wisse, P., and Karunarathna, H., 2015. Effects of storm clustering on beach/dune evolution. *Marine Geology* [online], 370, 63–75.

Hessner, K.; Reichert, K.; Nieto Borge, J. C.; Stevens, C. and Smith, M., 2014. High-resolution X-Band radar measurements of currents, bathymetry and sea state in highly inhomogeneous coastal areas. *Ocean Dynamics*, 64, 989-998.

Holman, R. A. and Stanley, J., 2007. The history and technical capabilities of Argus. *Coastal Engineering*, 54 (6–7), 477–491.

Karunarathna, H., Pender, D., Ranasinghe, R., Short, A. D. and Reeve, D. E., 2014. The effects of storm clustering on beach profile variability. *Marine Geology*, 348, 103–112.

Lamb, H.; Frydendahl, K., 2005. Historic Storms of the North Sea, British Isles and North-west Europe. Cambridge University Press. ISBN 0-521-61931-9.

Long, P.E. and Zalasiewicz, J.A., 2011. The molluscan fauna of the Coralline Crag (Pliocene, Zanclean) at Raydon Hall, Suffolk, UK: Palaeoecological significance reassessed. *Palaeogeography, Palaeoclimatology, Palaeoecology* 309, 53–72.

Pye, K. & Blott, S. J., 2006. Coastal processes and morphological change in the Dunwich-Sizewell area, Suffolk, UK. *Journal of Coastal Research*, 22, 453-473.

Reichert, K., Hessner, K., Nieto Borge, J. C., and Dittmer, J., 1999. WaMoS II: A radar based wave and current monitoring system. *Isope '99 Proceedings* Vol. 3, 3 (May), 1–5.

Young, I.R., Rosenthal, W., Ziemer, F., 1985. A three-dimensional analysis of marine radar images for the determination of ocean wave directionality and surface currents. *Journal Geophysical Research*. (90), 1049–1059.